 doi.org/10.52568/000647/JCSP/42.03.2020

Investigation of the Magnetic and Electronic Properties of Copper Nanocluster Cu_{14} Contaminated with Fe, Ni and Co

Maryam Darvishpour*, Mohammad Hossein Fekri
Department of Chemistry, Ayatollah Borujerdi University, Borujerd, Iran.
ma.darvishpour@gmail.com*; m.h.fekri@abru.ac.ir

(Received on 8th January 2018, accepted in revised form 2 August 2019)

Summary: We have presented density functional calculations of the electronic structures and magnetic properties of bimetallics nanoclusters $Cu_{14-n}M_n$ (n=1-3) (M=Fe, Ni and Co) in the FCC crystal structure. For the calculations of the physical properties of the compounds, we have used the full potential linearized augmented plane wave method. The magnetic nature, semiconducting, half metallicity and metalloid of transition metals clusters in the FCC crystal structure are investigated. Results show that studied systems have ferromagnetic properties against Cu_{14}Cluster. It is found that band gap of the clusters decreases with doping of atoms compared to pure cluster $Cu_{14,}$ Particularly for Fe. These calculations show that Cu_{14} and $Cu_{12}Co_2$ are metals, while $Cu_{13}Fe$, $Cu_{12}Fe_2$, $Cu_{13}Co$, $Cu_{11}Co_3$ and $Cu_{11}Ni_3$ are half-metals and $Cu_{11}Fe_3$ and $Cu_{12}Ni_2$ are metalloid. Between these clusters, $Cu_{13}Ni$ is semiconductor. The spin polarization and the magnetic moment of the systems are dependent on number and type of the host transition metal atoms. The $Cu_{13}Ni$ has maximum spin polarization and stability. These results provide a new candidate for applications this series of compounds as dilute magnetic clusters and half-metal in spintronic devices.

Keywords: Bimetallic clusters, Transition metal, Magnetic properties, Half metallicity, Spintronic

Introduction

For the design of feasible electronic devices, defects and impurities have been used to adjust the electrical, optical, and other properties. Dilute Magnetic Semiconductors (DMSs) are usually designed by inserting transition metal (TM) impurities into the non-magnetic semiconductors [1, 2]. Stimulating effects in this materials category, such as exciton spin polarization and spin-polarized electrical current, which gives rise to potential applications in spintronics [3]. Magnetic and electronic properties in semiconductors are usually dependent to unfilled 3d electron shells of TM ions embedded in the guest site. These aspects open up the possibility that the magnetic behavior of the materials can be controlled indeed by changing the vehicle density [4]. Derby et al. [5] studied global minima for Cu_n, Au_n and their alloy clusters in the size range $n \leq 55$. These kinds of empirical methods are found to be good to predict the global minima of the clusters but cannot predict electronic properties such as shell closing effect for n = 2, 8, 18, 20, 40, ..., HOMO-LUMO gap energies and ionization potentials.

As is well known, the valence electrons of Cu 4*s* are free-electron like, the stability of small Cu_nclusters can thus be explained by the Jellium model [6,7].What's more, it is well known that the Kondo effect [8] can be observed at low temperature, if a magnetic impurity such as Fe, Co or Ni is doped in a free-electron-like metal, such as Cu.

Consequently, it is interesting to investigate the interaction of a transition metal (TM) atom with Cu in the nanoscale and creating of bimetallic compounds [9-11]. There are various structures of Cu clusters, such as face center cubic (FCC) and icosahedral.

In this work, we focus on substitution 3d TM impurities (TM= Fe, Ni and Co) in Cu_{14} cluster (FCC) to investigate their dilute magnetic characters and half-metal properties. Transition metal ions were implanted into Cu_{14}cluster with the concentrations of 7, 14and 21%. Using first-principles density functional theory (DFT) calculations, we study the structural, electronic, and magnetic properties of substitution 3d TM impurities in these new bimetallic compounds. We present the geometry structures, gap energy, and magnetic properties of all the studied TM clusters and got interesting results. Novelty this work is demonstrates some of M_nCu_{14-n}clusters as ferromagnetic half- metals for design spintronic instruments.

Computational details

The present calculations are performed by using the full potential linearized augmented plane wave (FP-LAPW) method in the framework of the Density Functional Theory (DFT) [12], within the generalized gradient approximation (GGA) [13], implemented the WIEN2k code [9].We expand the

*To whom all correspondence should be addressed.

basis function up to $R_{mt}K_{max}$ =5, (R_{mt} is the least muffin-tin sphere radii, K_{max} is the maximum modulus for the reciprocal vectors), 200 k-points and G_{Max} = 14 are used.

Results and Discussion

Cu_{14} has a FCC geometry with 6 atoms in faces, 8 atoms in vertices that are symmetrically equivalent. In order to handle the large number of homologs [14], we started off our geometry optimization of $Cu_{14-n}M_n$ (n = 1- 3) with $Cu_{13}M$ and increased the number of dopants. For $Cu_{13}M$, we can be replaced one of Cu_{14} atoms with M on two possible sites, on a face or on vertices. As expected, homolog one had lower energies for all the TM elements [15]. Hence we selected first state (atom 1). The second M can then be placed on any of another vertices or faces. We select second and third atoms in adjacent position (atom 2 and 11).We optimized nine possible face center cubic structures as shown in Fig. 1. The structural stability of Cu_{14-n} M_n (n=1-3) clusters have been studied for all compositions. For each cluster and composition of them, face center cubic isomer of Cu_{14} and doped compositions were relaxed without any constraints of symmetry.

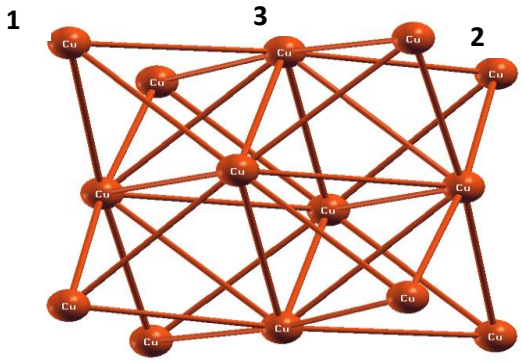

Fig. 1: $Cu_{14-n}M_n$ (n=1-3) clusters. Three labeled Cu atoms are substituted by M= (Fe, Co, Ni).

Electronic band gaps and structural parameters such as magnetic momentum, Fermi energy and total energy for Cu_{14} and Cu_{14-n} M_n (n=1-3) clusters in FCC phase are calculated. Density of state (DOS) essentially reflects optoelectronic properties and hence there is an effective tool for studding these optical materials. The results of optimization varied according to the size of the elements. The lighter ones, Sc, Ti, and V resulted in distortion from FCC symmetry, with bond breaking between the neighboring M atoms that opened up the structure. So these elements were ruled out. The rest of the 3d TM elements resulted in slight distortions, with minor changes in bond lengths, of the FCC, including the homologs with higher energies. The energy structures for M = Fe, Co, and Ni is the lowest and total magnetic moments is the highest.

Electronic band gaps and structural parameters such as total energy, Fermi energy, magnetic momentum and Energy gap for $Cu_{14-n}M_n$ (n=1-3) clusters in FCC phase are calculated (Table-1). Table show that total energy for $Cu_{13}Fe$, $Cu_{12}Fe_2$ and, $Cu_{11}Fe_3$ are -45569.677789, -44805.322326 and -44041.950868 Ry, respectively. These data are expressed that stability of pure cluster (Cu_{14}) decrease with doping, also stability decreases with increasing doping concentration but stability is still a big deal. The table shows that total energy for $Cu_{13}Co$, $Cu_{12}Co_2$ and, $Cu_{11}Co_3$ are -45787.238318, -45264.212396 and -44763.322274 Ry, respectively. These data express that stability of pure cluster (Cu_{14}) decrease with doping, also with increasing of doping concentration decrease stability. By comparing these values with total energy of $Cu_{14-n}Fe_n$(n=1-3) clusters, we find that the substitution of cobalt instead of copper atoms in the parent cluster will lead to further instability. Total energy for $Cu_{14-n}Ni_n$ (n=1-3) clusters in face center cubic phase are calculated (Table-1). Table shows that total energy for $Cu_{13}Ni$, $Cu_{12}Ni_2$ and, $Cu_{11}Ni_3$ are -46067.596219, -45796.792376 and -45529.955196 Ry, respectively. These data are expressed that stability of pure cluster (Cu_{14}) decreases with doping, also with increasing of doping, concentration decreases stability. By comparing these values with total energy of $Cu_{14-n}Fe_n$ (n=1-3) and $Cu_{14-n}Co_n$ (n=1-3) clusters, we find that stability trend for three atoms of doping as follow: Ni> Co> F

Fig. 2 shows that calculated band gap varies at different concentrations of TM. The calculated direct Energy gap of pure Cu_{14} is 0.68eV. Data show band gap decreases with doping of cluster. The reduction in the band gaps is due to the presence of local strains and local electric fields generated by TM atoms. Also, results show that band gap increases as the concentration of TM= Fe, Co increases. The variation in band gap strongly depends upon the TM/Cu concentration in $Cu_{14-n}TM_n$. These results provide a promising way for band gap engineering of devices based on Cu_{14} cluster. Thus, varying the TM/Cu concentration photonic devices in various region of the spectrum can be constructed. In the other hand, results show band gap energy of $Cu_{13}Ni$, $Cu_{12}Ni_2$ and $Cu_{11}Ni_3$ is determined 0.0240, 0.0045 and 0.089 Ry, respectively. This result show that this graph does not follow any particular trend.

e

Table-1: Electronic and magnetic properties of clusters $Cu_{14-n}M_n$ (n=1-3).

Cluster	Total energy (Ry)*	Fermi energy (Ry)	Total Spin magnetic momentum in cell(μB)	Energy Gap (Ry)
Cu_{14}	-46310.321023	-0.32210	-0.01	0.0493
$Cu_{13}Fe$	-45569.677789	-0.28108	3.00	0.0007
$Cu_{12}Fe_2$	-44805.322326	-0.28341	6.00	0.0066
$Cu_{11}Fe_3$	-44041.950868	-0.27032	9.00	0.0097
$Cu_{13}Co$	-45787.238318	-0.30971	2.00	0.0266
$Cu_{12}Co_2$	-45264.212396	-0.29261	3.79	0.0183
$Cu_{11}Co_3$	-44763.322274	-0.27787	6.00	0.0070
$Cu_{13}Ni_1$	-46067.596219	-0.28296	0.98	0.0240
$Cu_{12}Ni_2$	-45796.792376	-0.28680	2.00	0.0045
$Cu_{11}Ni_3$	-45529.955196	-0.28326	3.02	0.0089

* 1Ry= 13.6 eV

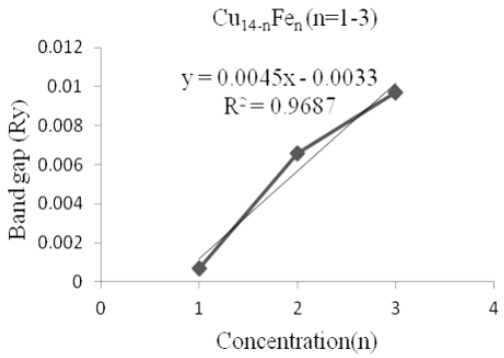

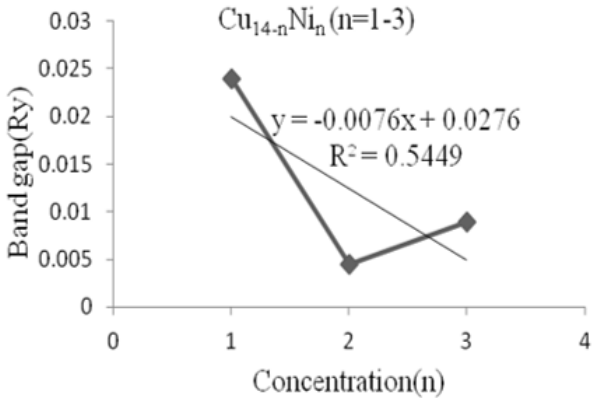

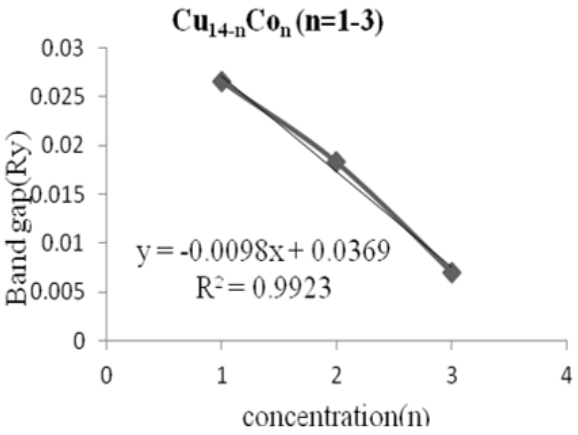

Fig. 2: Plot of changes in number of atoms against the band gap in Cu_{14-n} M_n (n=1-3).

For metallic cluster of Cu_{14}, density of states (DOS) in the vicinity of the Fermi level is important as it is responsible for chemical reactivity. For comparing the effect of doping, we plotted the pure Cu_{14} spin polarized total DOS at first. As seen in Fig. 3, the majority and minority channels of Cu_{14} have equal states for states of below the Fermi level and vice versa above the Fermi level. As the doping concentration is increased, the Van Hove singularities have broadened, with the magnitude of the peaks decreasing for some or remaining constant for others. This indicates change in the distribution of the DOS, the availability of more states with wider range of energies, not just those near the peaks.

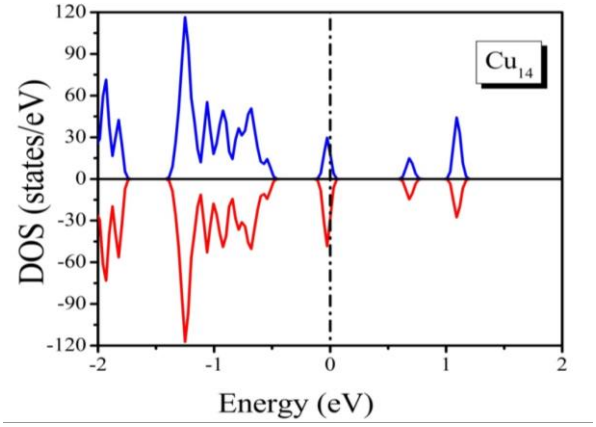

Fig. 3: DOS plot of Cu_{14} cluster.

The DOS of the bimetallic clusters are quite different from that the parent structure (Cu_{14}) without doping. The changes in DOS are seen across the spectrum. Cu_{14} nanocluster is anti-ferromagnetic metal. While clusters contain of Fe, Co and Ni are ferromagnetic. It is not surprising then that the effect of these elements as doping on the DOS of the cluster Cu_{14} be quite different from that of another TM in first row of periodic table. Finally, the FCC symmetry of Cu_{14} is broken very slightly due to very minor changes in bond lengths at the range of doping concentration considered in this work, therefore, we will not consider the John–Teller effect.

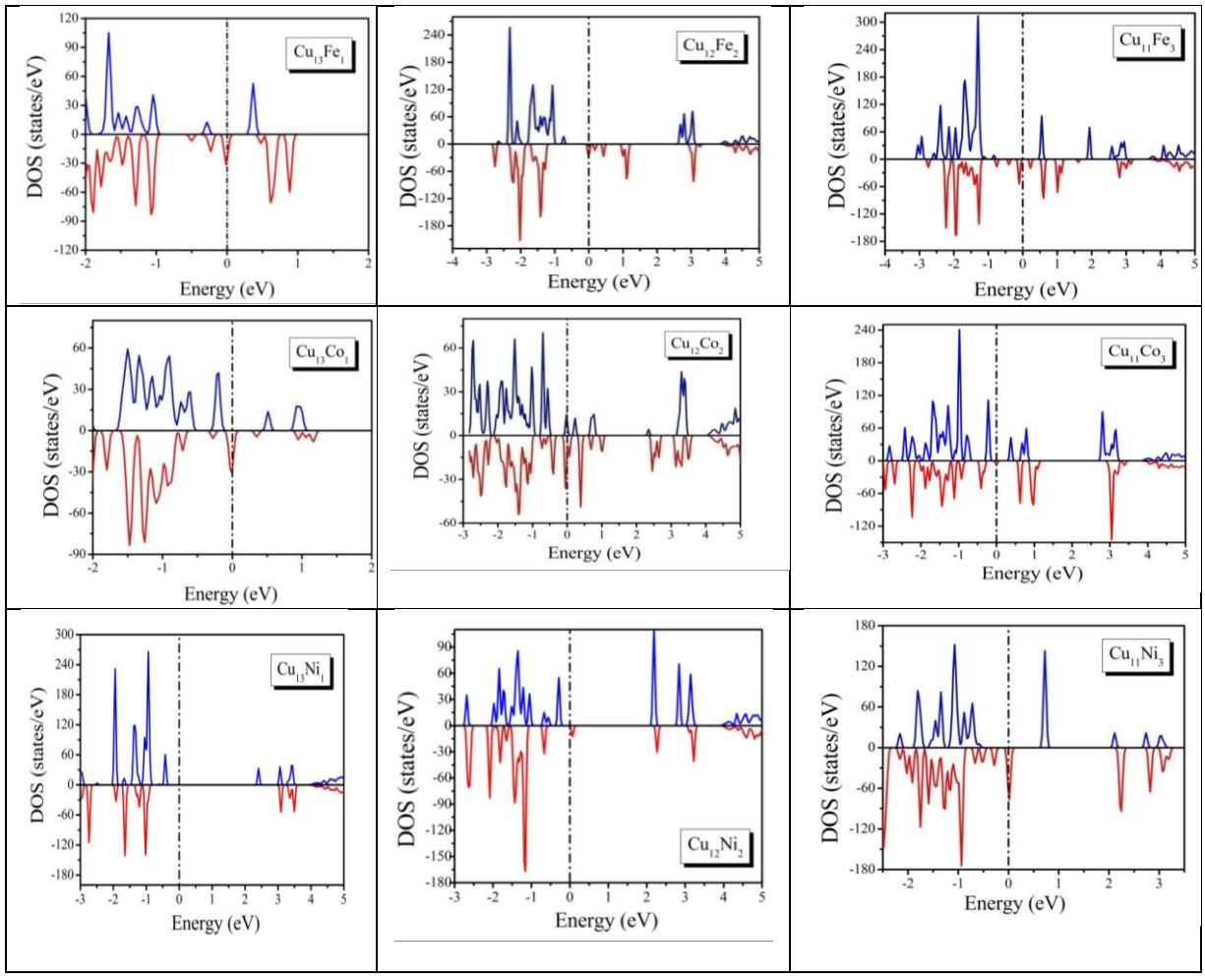

Fig 4. DOS plot of Cu_{14-n} M_n (n=1-3).

Adamowicz and Wierzbicki [16] suggested that only the minority spin (↓) active state cause's global magnetic moment. Magnetic momentum in atoms (MMI) and total valence charge (CHA) cluster $Cu_{14}$and bimetallic clusters$Cu_{14-n}M_n$ (n=1-3) are shown in(**S1-S7**).

Total Spin magnetic momentum for $Cu_{13}Fe$, $Cu_{12}Fe_2$ and $Cu_{11}Fe_3$ are 3.00, 6.00 and 9.00 respectively (Table-1). These results show that total spin magnetic momentum for $Cu_{14-n}Fe_n$ (n=1-3) clusters are very higher than pure Cu_{14} cluster. Also, total spin magnetic momentum increases with increasing of doping concentration. Magnetic momentum in atoms (MMI) for $Cu_{14-n}Fe_n$(n=1-3)(μB) (**S2**)admits that increasing in total spin magnetic momentum is due to high magnetic momentum in doping atoms. Total valence charge in atoms for $Cu_{14-n}Fe_n$ (n=1-3) provided in **S3** that show valence charge for doping atoms is3 units lower than Cu atoms.

Density of states $Cu_{14-n}Co_n$(n=1-3) is shown in Fig. 4. Overall half- metallicity is a property that compound is conductor in one spin- state (↓) and semiconductor in the other spin state (↑), that confirmed for $Cu_{13}Co$ and $Cu_{11}Co_3$ clusters.The nature of $Cu_{12}Co_2$ cluster is different than the rest of the two because valence and conduction bands of this compound crosses each other for majority spin- state (↑) and the bottom of the conduction band crosses the Fermi level for minority spin-state (↓). Hence $Cu_{12}Co_2$ cluster is metallic for both spin-channels. It can also be noted from the majority spin- states (↑) that conduction band and valence band states overlap and there is no forbidden energy gap at the Fermi level. These completely filled bands, in which conduction and valance band states overlap around the Fermi level are mainly due to the Fe-3d and Cu-2p states. While cut offs at the Fermi level can be seen for the majority spin-states (↑) of $Cu_{13}Co$and $Cu_{11}Co_3$, and hence for both compounds forbidden energy gaps exist at the Fermi level. Finally, due to differences in the density of states up and down relative to each other, these tree compounds are ferromagnetism.

Magnetic momentum in atoms (MMI) for $Cu_{14-n}Co_n$ (n=1-3) are presented in **S4**. Total spin magnetic momentum for $Cu_{13}Co$, $Cu_{12}Co_2$ and $Cu_{11}Co_3$ are 2.00, 4.00, 6.00 μB, respectively (Table 1). These results show that total spin magnetic momentum for Cu_{14-n} Co_n (n=1-3) cluster is very higher than pure Cu_{14} cluster, also, total spin magnetic momentum increase with increasing doping concentration. It admits that increasing in total spin magnetic momentum is due to high magnetic momentum in doping atoms. Total valence charge in atoms for $Cu_{14-n}Co_n$(n=1-3) provided in **S5** that show valence charge for doping atoms is2 units lower than Cu atoms.

Fig. 4 show that there are not the density of state at Fermi level for $Cu_{14-n}Ni_n$ (n=1-2) cluster. Hence for both compounds forbidden energy gaps exist at the Fermi level. In $Cu_{12}Ni_2$ cluster, minority states spin down crosses Fermi level at zero value, so this compound is ferromagnetic metalloid but $Cu_{13}Ni$ cluster is a ferromagnetic semiconductor.

The Fig. 4 shows that the spin down (↓) state contains a greater number of electrons than the spin up (↑) state. The results also reveal that a band gap exists around the Fermi level for the spin up state, while for the spin down state some of the valance bands crosses the Fermi level and are relocated to the conduction band. Based on the above discussion, $Cu_{11}Ni_3$ is half - metal. It is also evident from the spin up state of the figure that in the vicinity of the Fermi level all the Ni-3d states are empty. The nature of attraction in these dilute magnetic semiconductors can be described by the spd exchange splitting.

Magnetic moments for $Cu_{14-n}Ni_n$ (n=1-3) clusters are presented in **S6**. The main source of magnetization in these materials is unfilled Ni-3d states. It is clear that total magnetic moment for $Cu_{11}Ni_3$ is larger than $Cu_{12}Ni_2$ and $Cu_{13}Ni$. The origin of the Ni magnetic moment can be related to the partially filled e.g. level in the 3d state [17]. The negative values of the moments at table demonstrate that induced moments on these atoms are anti-parallel to Ni atoms and interact anti-ferromagnetically, while the positive values of the magnetic moment of Cu indicates parallel magnetic moment to Ni. Total valence charge in atoms for $Cu_{14-n}Ni_n$(n=1-3) provided in **S7** that show valence charge for doping atoms is0.7 units lower than Cu atoms.

Conclusion

In this research, we have presented density functional calculations of the structural electronic and magnetic properties of nanoclusters $Cu_{14-n}M_n$ (n=1-3) that M=Fe, Co and Ni in the FCC crystal structure. For calculations of the physical properties of compounds, we have used FP-LAPW method. It is found that band gap of the materials decreases with increase in doping atoms compared to pure cluster Cu_{14}, particularly for Fe doping. A maximum value of 0.68 eV is determined for the band gap of pure cluster, which reaches a minimum value of 0.01 eV when one atom is replaced by Fe in Cooper Cluster. Band gap increases with the increase in Fe number of atoms and

decreases with the increase in Co number of atoms. For Ni doping does not follow any particular trend.

The magnetic nature, semiconducting, half metallicity and metalloid of TM doped Cu_{14} cluster in the FCC crystal structure are investigated. These calculations show that Cu_{14} and $Cu_{12}Co_2$ are metal, while $Cu_{13}Fe$, $Cu_{12}Fe_2$, $Cu_{13}Co$, $Cu_{11}CoandCu_{11}Ni_3$ are half-metal, $Cu_{11}Fe_3$ and $Cu_{12}Ni_2$ are metalloid. Between these clusters, $Cu_{13}Ni$ is semiconductor. For minority spin channels the electronic cloud of the Fe/Co/Ni-p states overlaps with the TM-3d and 2s state and causes spd-hybridization. The spd-hybridization in these compounds is responsible for the half-metallicity.

References

1. Y. Feng, W. X. Ji, B. J. Huang, X. L. Chen, F. Li, P. Li, C. W. Zhang, P. J. Wang The magnetic and optical properties of 3d transition metal doped SnO2 nanosheets. *RSC Adv*, **5**, 24306 (2015).
2. Z. L. Zhu, W. G. Chen, Q. Sun, Y. Jia Half-metal behaviour mediated by self-doping of topological line defect combining with adsorption of 3d transition-metal atomic chains in graphene. *J Phys D*, **47**, 055303 (2014).
3. K. Sato, L. Bergqvist, J. Kudrnovsk´y, P. H. Dederichs, O. Eriksson, I. Turek, B. Sanyal,G. Bouzerar,H. atayama-Yoshida, V. A. Dinh, T. Fukushima, H. Kizaki, and R. Zeller, *Rev. Mod. Phys*. **82**, 1633 (2010).
4. M. Shahjahan, M. J. Sadique, Stable dilute magnetic semiconductor and Curie temperature of 3d transition metal doped strontium titanate perovskite material *Computational Condensed Matter* **14**, 89 (2018).
5. K. Mukul, M. Abhijit, A.K. Bhattacharya, Copper clusters: Electronic effect dominates over geometric effect *Eur. Phys. J. D*, **31**, 477–485 (2004).
6. S. Mingzhi, D. Ning, C. Hongshan, Study on the Geometric and Electronic Structures of Al_nSi_m (n= 3, 4, 5; m= 1, 2, 3, 4) Clusters, *J Clust Sci*, 141–150 (2018).
7. H. Tsunoyama, M. Akutsu, K. Koyasu, A. Nakajima, The stability of binary $Al_{12}X$ nanoclusters (X = Sc and Ti): superatom or Wade's polyhedron, *Journal of Physics: Condensed Matter*, **30**, 494004 (2018).
8. A. N. Néel, J. Kröger, R. Berndt, T. O. Wehling, A. I. Lichtenstein, and M. I. Katsnelson Controlling the Kondo Effect $CoCu_n$ in Clusters Atom by Atom *Phys. Rev. Lett*. 101, 266803 (2008).
9. C. S. Cutrano, Ch.E. Lekka, Structural, magnetic and electronic properties of Cu-Fe nanoclusters by density functional theory calculations, *Journal of Alloys and Compounds*, **707**, 114 (2017).
10. B. F. Berthier, Magic Numbers for Bimetallic Clusters, *Solid State Phenomena*, **172**, 1038 (2011).
11. Y. C. Gao, Y. Zhang, X. T. Wang, Phase stability, band gap, and electronic and magnetic properties of quaternary heusler alloys FeMnScZ (Z = Al, Ga, In), *J. Korean Phys.Soc*., **66**, 959 (2015).
12. L. Peters, E. Şaşıoğlu, I. Mertig, M. I. Katsnelson, Ab initio study of the Coulomb interaction in Nb_xCo clusters: Strong on-site versus weak nonlocal screening, *Phys. Rev. B*, 97, 045121 (2018).
13. T. Yu,Y.Gao, D. Xu, Z Wang, Actinide endohedral boron clusters: A closed-shell electronic structure of $U@B_4$, *Nano Research* **1**, 354 (2018).
14. K. b. Schwarz, P. Blaha, G, .K. H. Madsen Electronic structure calculations of solids using the WIEN2k package for material sciences, *Comp. Phys. Comm.*, **147**, 71 (2002).
15. G. H. Guvelioglu, P. Ma, X. He, R. C. Forrey and C. H., First principles studies on the growth of small Cu clusters and the dissociative chemisorption of H_2, *Phys. Rev. B*, **73**, 155436 (2006).
16. L. Adamowicz and M. Wierzbicki, Symmetry Induced Half-Metallic Alkaline Earth Ferromagnets, *Acta Phys. Pol. A*, **115**, 217 (2009).
17. Y. Kwon, A. Ilyin and O. Nazarenko, Electric explosion of wires in multicomponent reactionary liquid ambiences as method for producing nanopowder of complex composition, in Proceedings of the 9th Russian-Korean International Symposium on Science and Technology (2005).